Effect of Conformational Changes on a One-Electron Reduction Process: Evidence of a One-Electron P–P Bond Formation in a Bis(phosphinine)

Sylvie Choua,[a] Cosmina Dutan,[a] Laurent Cataldo,[a] Théo Berclaz,[a] Michel Geoffroy,*[a] Nicolas Mézailles,[b] Audrey Moores,[b] Louis Ricard,[b] and Pascal Le Floch*[b]

Abstract: EPR spectra show that one-electron reduction of bis(3-phenyl-6,6-(trimethylsilyl)phosphinine-2-yl)dimethylsilane (**1**) on an alkali mirror leads to a radical anion that is localized on a single phosphinine ring, whereas the radical anion formed from the same reaction in the presence of cryptand or from an electron transfer with sodium naphthalenide is delocalized on the two phosphinine rings. Density functional theory (DFT) calculations show that in the last species the unpaired electron is mainly confined in a loose P–P bond (3.479 Å), which results from the overlap of two phosphorus p orbitals. In contrast, as attested by X-ray spectroscopy, the P–P distance in neutral **1** is large (5.8 Å). As shown by crystal structure analysis, addition of a second electron leads to the formation of a classical P–P single bond (P–P 2.389 Å). Spectral modifications induced by the presence of cryptand or by a change in the reaction temperature are consistent with the formation of a tight ion pair that stabilizes the radical structure localized on a single phosphinine ring. It is suggested that the structure of this pair hinders internal rotation around the C–Si bonds and prevents **1** from adopting a conformation that shortens the intramolecular P–P distance. The ability of the phosphinine radical anion to reversibly form weak P–P bonds with neutral phosphinines in the absence of steric hindrance is confirmed by EPR spectra obtained for 2,6-bis(trimethylsilyl)-3-phenylphosphinine (**2**). Moreover, as shown by NMR spectroscopy, in this system, which contains only one phosphinine ring, further reduction leads to an intermolecular reaction with the formation of a classical P–P bond.

Keywords: aromaticity · density functional calculations · electron transfer · EPR spectroscopy · fluxionality · P ligands

Introduction

Topological modifications that accompany electron-transfer processes are currently attracting extensive interest.[1] These modifications involve various fields of chemistry, such as biochemical mechanisms, and molecular recognition, and are also investigated in the context of molecular electronics and sensors because they are expected to yield switchable molecular systems.[2] Unfortunately, electron-transfer reactions are often complex. For example, reduction of aromatic molecules by an alkali metal mirror gives rise to several types of ion pairs and aggregates.[3] Therefore, it is important to determine the factors that govern the selective formation of a reduction compound. The conformation of the electron-acceptor system is expected to play a crucial role because in the first step it can affect the distance between the reductant and the reduction site, while in the second step it can stabilize the reduction species by allowing the additional electron to be delocalized better.

We have recently shown that the one-electron reduction of some macrocyclic species can lead to an appreciable interaction between two aromatic subunits. As a result, a large delocalization of the unpaired electron over the whole molecule occurs and a marked change in the macrocyclic structure is observed.[4] In particular, incorporation of two phosphinine rings into a macrocycle forces the radical anion to adopt a conformation that allows the formation of a rare phosphorus–phosphorus one-electron bond.[5,6] Recently, Hoeffelmeyer and Gabbaï have shown that the sterically congested structure of 1,8-bis(diphenylboryl)naphthalene

[a] Dr S. Choua, C. Dutan, Dr L. Cataldo, Dr T. Berclaz, Prof. M. Geoffroy
Department of Physical Chemistry, University of Geneva
30 Quai Ernest Ansermet, 1211 Geneva 4 (Switzerland)
Fax: (+41) 022-379-65-52
E-mail: michel.geoffroy@chiphy.unige.ch

[b] Dr N. Mézailles, A. Moores, Dr L. Ricard, Prof. P. Le Floch
Laboratoire "Hétéroéléments et Coordination"
UMR CNRS 7653, Département de Chimie, Ecole Polytechnique
91128 Palaiseau Cedex (France)
Fax: (+33) 169-33-39-90
E-mail: lefloch@poly.polytechnique.fr

Supporting information for this article is available on the WWW under http://www.chemeurj.org/ or from the author.

DOI: 10.1002/chem.200400073

leads to the formation of a boron–boron one-electron bond upon reduction.[7]

In the present study, our purpose is to investigate the effect of geometric constraints on the outcome of a reduction. A system that is able to adopt several conformations, and thus potentially lead to different relative orientations of the reduction centers, was chosen. Molecule **1**, which contains two phosphinine rings linked by an sp^3 silicon atom, possesses the desired features for such an investigation. Indeed, the two reduction centers of the molecule, namely the two phosphinine rings, may accommodate different relative orientations between two limiting geometrical structures **1a** and **1b**.

In this approach, structural information is obtained from EPR spectra for the paramagnetic species and from X-ray diffraction data and NMR spectra for the diamagnetic compounds. Most of these structures are also discussed in the light of DFT calculations. Interpretations of the EPR spectra obtained for the one-electron reduction species $\mathbf{1}^{\bullet-}$ rely, in part, on the analysis of the spectra recorded after reduction of monophosphinine **2** (which models half of **1**), which was also investigated in the present study. Comparisons have also been made with the results previously reported for macrocycle **3**.[5]

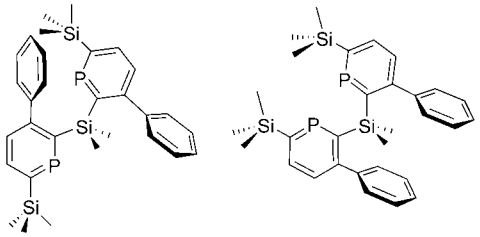

1a **1b**

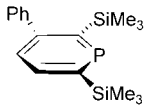

2

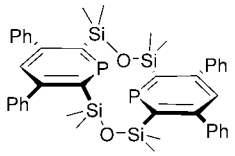

3

Abstract in French: *Les spectres RPE montrent que la réduction monoélectronique du bis(3-phenyl-6,6(trimethylsilyl)-phosphinine-2-yl)dimethylsilane (**1**) sur miroir de potassium conduit à un radical anion localisé sur l'un des deux cycles phosphinine alors que dans le radical anion obtenu par réaction identique en présence de cryptant ou par transfert électronique du naphthalènure de sodium, l'électron non apparié est délocalisé sur les deux cycles phosphinine. Des calculs DFT confirment que cet électron se situe principalement dans une liaison P–P assez longue (3.479 Å) résultant du recouvrement des orbitales p des deux atomes de phosphore. A titre de comparaison la distance P–P dans le composé neutre a été mesurée à 5.8 Å par spectroscopie RX. La réduction par un second électron conduit à la formation d'une liaison P–P classique, comme l'atteste la structure RX (P–P = 2.389 Å). Les modifications observées en RPE en présence de cryptant ou en changeant la température réactionnelle corroborent l'hypothèse de la formation d'une paire d'ions qui stabilise la structure radicalaire localisée sur un cycle. La présence de cette paire d'ions qui rend difficile la rotation autour du lien inter-phosphinine, pourrait expliquer l'impossibilité pour le composé **1** d'adopter une conformation où les atomes de phosphore sont proches. La possibilité pour un anion de phosphinine de former de façon réversible une liaison faible P–P avec une phosphinine neutre en l'absence de contrainte stérique a été mise en évidence par l'étude RPE du composé 2,6-bis-trimethylsilyl-3-phenyl-phosphinine (**2**). Par ailleurs, il a été montré par RMN que la réduction de monophosphinines de ce type conduisait, via une réaction intermoléculaire, à la formation de liaisons P–P classiques.*

Results

Neutral species: synthesis, NMR spectra, and crystal structure

Monophosphinine 2: Monophosphinine **2** was synthesized according to the diazaphosphinine method developed several years ago in our laboratory,[8] and relies on the high reactivity of 1,3,2-diazaphosphinine **4** with alkynes. In the first step, compound **4** is allowed to react with one equivalent of trimethylsilylphenylacetylene in a [4+2]/retro [4+2] sequence to give 1,2-monoazaphosphinine **5** (Scheme 1). Although compound **5** was not isolated, its formation was established by ^{31}P NMR spectroscopy. Compound **5** was then allowed to react with trimethylsilylacetylene in another [4+2]/retro [4+2] sequence to yield the desired asymmetric phosphinine **2** in good yield. Compound **2** was isolated as a white solid and its formulation was proven by usual NMR techniques as well as elemental analysis.

Bis(phophinine) 1: Bis(phosphinine) **1** was synthesized by using a previously reported method.[9] The room-temperature ^{31}P NMR spectrum exhibits only one signal; this suggests that the phosphinine subunits undergo fast rotation around the C5–Si2 and C6–Si2 bonds. Lowering the temperature to −95 °C did not induce broadening of the peak either in the ^{31}P or ^{1}H NMR spectrum, and this indicates that the rotational barrier is very low. Therefore, we were interested to see which of the two conformers would be favored in the solid state. Single crystals were grown by slow diffusion of methanol into a solution of **1** in toluene. The results of the X-ray crystal analysis are shown in Figure 1. Significant geometrical parameters and crystal data are gathered in Table 1 and 2. In the solid state, the most stable conformation is closer to **1a**, since the two phosphinine planes are perpendicular to each other (91.59°). The C5-Si2-C6 angle shows that the system is not strained (111.85(7)°). In this conformer the interphosphorus distance is particularly

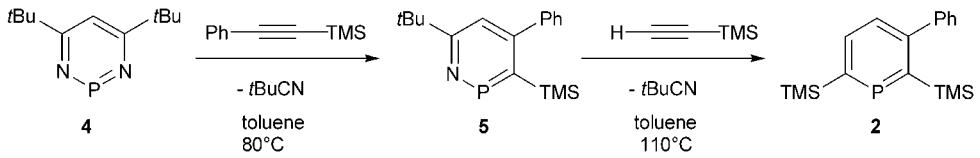

Scheme 1. Synthesis of compound **2**.

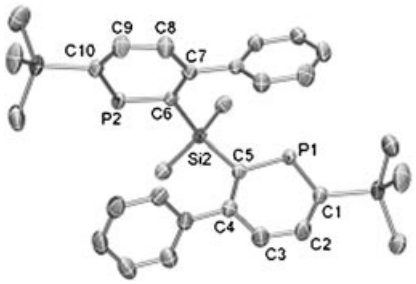

Figure 1. Structure of neutral compound **1** (ORTEP view). The numbering is arbitrary and different from that used in the assignment of the NMR data.

Table 1. Selected bond lengths [Å] and angles [°] for **1**.

P1–C1	1.730(2)	P1–C5	1.743(2)
P2–C10	1.728(2)	P2–C6	1.742(2)
Si2–C5	1.893(2)	Si2–C6	1.896(2)
C1–C2	1.393(2)	C2–C3	1.384(2)
C3–C4	1.393(2)	C4–C5	1.409(2)
C6–C7	1.404(2)	C7–C8	1.400(2)
C8–C9	1.387(2)	C9–C10	1.395(2)
C10-P2-C6	105.10(7)	C1-P1-C5	104.84(8)
C2-C1-P1	121.1(1)	C5-Si2-C6	111.85(7)
C2-C3-C4	124.4(2)	C3-C2-C1	124.9(2)
C4-C5-P1	121.9(1)	C3-C4-C5	122.7(2)
C4-C5-Si2	123.6(1)	P1-C5-Si2	114.4(1)
C7-C6-P2	121.9(1)		

Table 2. Crystal data and structural refinement details for the structure of compound **1** and $[\mathbf{1}]^{2-}\cdot 2\,Na^{+}$.

Compound	**1**	$[\mathbf{1}]^{2-}\cdot 2\,Na^{+}$
formula	$C_{30}H_{38}P_2Si_3$	$C_{38}H_{57}Na_2O_2P_2Si_3$
M_r	544.81	738.03
crystal size [mm]	$0.30\times0.30\times0.20$	$0.22\times0.16\times0.16$
crystal system	monoclinic	triclinic
space group	$P2_1/c$	$P\bar{1}$
a [Å]	17.334(5)	12.974(5)
b [Å]	20.775(5)	12.976(5)
c [Å]	17.415(5)	14.390(5)
α [°]	90.000(5)	112.060(5)
β [°]	100.400(5)	103.570(5)
γ [°]	90.000(5)	93.600(5)
V [Å^3]	6168(3)	2151.7(14)
Z	8	2
ρ_{calcd} [g cm^{-3}]	1.173	1.139
$F(000)$	2320	790
μ [cm^{-1}]	0.275	0.234
T [K]	150.0(10)	150.0(10)
θ_{max}	30.02	27.48
GOF	1.062	1.010
reflections measured	29546	14353
independent reflections	17988	9822
R_{int}	0.0256	0.0253
reflections used	12563	7606
parameters refined	647	480
R_1[a]	0.0438	0.0460
wR_2[b]	0.1282	0.1263
difference peak/hole [e Å^{-3}]	0.466(0.060)/ −0.410(0.060)	0.637(0.054)/ −0.394(0.054)

[a] $R_1=\Sigma\,||F_o|-|F_c||/\Sigma\,|F_o|$. [b] $wR_2=[(\Sigma w(|F_o|-|F_c|)^2/\Sigma w\,|F_o|^2)]^{1/2}$.

large (5.8 Å). Distances and angles within the phosphinine rings are in the normal range and do not deserve any further comment.

Identification and structure of the dianionic species

Formation of a dimeric dianion by reduction of monophosphinine 2: Reduction of **2** at room temperature with one equivalent of sodium naphthalenide afforded a very moisture-sensitive green solution. The ^{31}P NMR spectrum of the crude mixture indicated the formation of two diamagnetic species in a 1:4 ratio ($\delta=-77.12$ and -82.8 ppm, respectively). Formation of diamagnetic species is consistent with previous results; these show that reduction of symmetric phosphinines **6** affords dimer **7** by the creation of a P–P bond (Scheme 2).[5] X-ray structure analysis of compound **7** shows that two sodium counterions complete the structure by coordinating with the *para*-carbon atom of one phosphinine unit and the phosphorus atom of the other

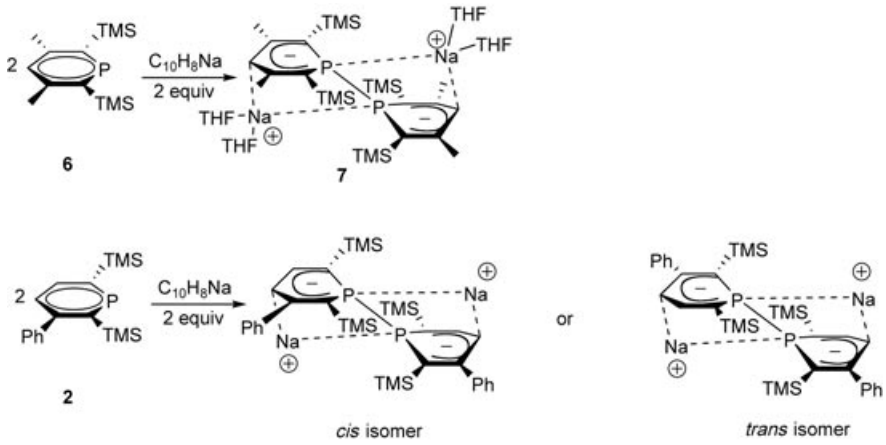

Scheme 2. Synthesis and conformation of the dimeric dianions formed by reduction of monophosphinines.

phosphinine unit. As the ^{31}P NMR signal for **7** is in the same region ($\delta = -68.5$ ppm) as the signal observed after the reduction of **2**, we postulated that the same type of structure was present in the solution of **2** following the reduction. However, the unsymmetrical nature of **2** (only one Ph group *meta* to P) affords *cis* and *trans* isomers $[\mathbf{2}_2]^{2-}\cdot 2Na^+$ (Scheme 2).

Formation and crystal structure of the bis(phosphinine) dianion $\mathbf{1}^{2-}$: Consistent with the above mentioned results, the reaction of bis(phosphinine) **1** in THF at room temperature with two equivalents of sodium naphthalenide afforded a burgundy-red solution whose NMR spectra indicated the formation of dianionic species $\mathbf{1}^{2-}$. Single crystals of this compound suitable for an X-ray diffraction study were grown at −18 °C, and the structure is shown in Figure 2, while significant geometrical parameters are given in Table 3. In contrast to the conformer of **1** (Figure 1), internal rotations around the C5–Si2 and C6–Si2 bonds in $\mathbf{1}^{2-}$ allowed the two phosphorus atoms to form a phosphorus–phosphorus bond (2.389 Å). In this structure, the phosphinine rings are almost planar (angle between the C1-P1-C5 and C1-C2-C4-C5 planes is 4.5°, while the corresponding angle for the second phosphinine is 3.0°). The C5-Si2-C6 angle is substantially smaller (98.96°) than that found in the neutral structure, and accounts for the cyclic strain within this molecule. The angle between the two phosphinine planes (48.16°) is also much smaller than in the neutral compound **1**. In $[\mathbf{1}]^{2-}\cdot 2Na^+$, the sodium cations stabilize the structure by coordinating to the phosphorus atom of one phosphinine unit as well as to the other phosphinine ring in a η^6-fashion (P2–Na1 2.818(1) Å, C1,C2,C3,C4,C5–Na1 range between 2.628 and 3.020 Å, P1–Na1 3.151(1) Å). One molecule of solvent (one molecule of diethyl ether for Na1, half a molecule of diethyl ether and half a molecule of THF for Na2) completes the coordination sphere of each sodium cation.

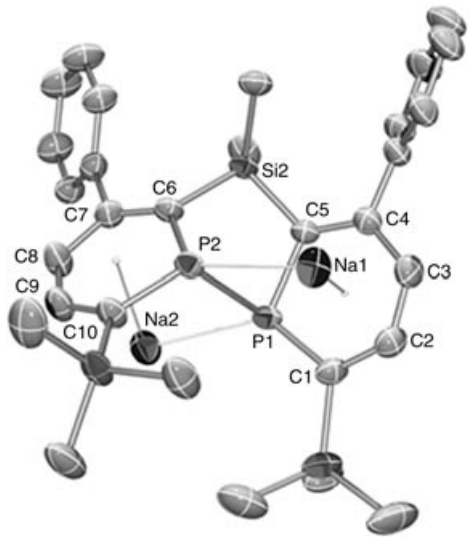

Figure 2. Structure of the dianionic compound $[\mathbf{1}]^{2-}\cdot 2Na^+$ (ORTEP view). The numbering is arbitrary and different from that used in the assignment of the NMR data. The diethyl ether and THF ligands coordinated to the sodium cations have been omitted for clarity.

Table 3. Selected bond lengths [Å] and angles [°] for $[\mathbf{1}]^{2-}\cdot 2Na^+$.

P1–C1	1.809(2)	P1–C5	1.837(2)
P1–P2	2.386(1)	P1–Na1	3.151(1)
P2–C10	1.800(2)	P2–C6	1.843(2)
P2–Na1	2.818(1)	Si2–C6	1.867(2)
Si2–C5	1.879(2)	Na(1)–C(3)	2.628(2)
Na(1)–C(2)	2.702(2)	Na(1)–C(4)	2.831(2).
C1-P1-C5	102.7(1)	C1-P1-P2	117.58(7)
C5-P1-P2	85.45(6)	C10-P2-Na1	129.87(6)
C6-P2-Na1	127.29(7)	P1-P2-Na	74.01(3)
C6-Si2-C5	98.96(8)		

EPR spectra of the monoanionic species

Spectra obtained after reduction of monophosphinine 2: A solution of **2** in THF (10^{-2} M) and in the presence of cryptand was reduced at room temperature with sodium naphthalenide and was then rapidly cooled to 200 K. At this temperature, the EPR spectrum contained a doublet (splitting: 42 G) of poorly resolved doublets.[10] Therefore, the solution was cooled to 120 K. The resultant frozen solution spectrum is shown in Figure 3a and is characterized by two external lines marked A and separated by 145 G, and by a central triplet marked B (coupling constant 31 G). The sample was then carefully heated and spectra were recorded at various temperatures. The spectra were particularly temperature sensitive between 160 and 200 K. The above-mentioned doublet (42 G) was clearly detected above 200 K and, as shown in Figure 3b, the spectra at 245 and 300 K exhibit a well-resolved structure (6 G) with an additional spin 1/2 nucleus. The sample

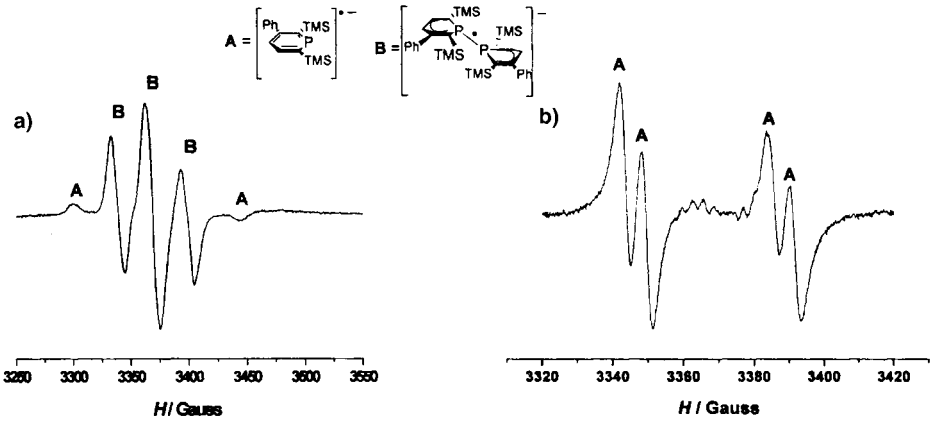

Figure 3. EPR spectra obtained after reduction of a solution of **2** at room temperature with Na naphthalenide in the presence of cryptand: a) frozen solution spectrum (120 K); and b) liquid solution spectrum (245 K).

was then cooled once again and showed that the temperature dependence of the spectra is reversible.[11]

The same liquid-phase spectrum was also obtained upon reduction of **2** with sodium naphthalenide in the absence of cryptand in a THF solution.[12]

EPR spectra obtained after reduction of bis(phosphinine) 1: *Reduction on a potassium mirror at 200 K in the absence of cryptand*: The spectrum recorded at 200 K (Figure 4a) consists of a rather broad doublet (large splitting, $A_{iso}=39.5$ G) and is similar to the spectrum recorded at the same temperature after reduction of **2**. However, at 95 K the spectrum (Figure 4b) drastically differs from the frozen solution spectrum obtained for **2**. An optimization program was used to find the parameters that would give rise to a satisfactory simulation of this spectrum (Figure 4b′),[13] and these parameters are reported in Table 4. The large "parallel" element ($T_{\parallel}=A_{iso}+\tau_3=140$ G) of the axial ^{31}P hyperfine tensor leads to the external signals marked A1 and A2, while the small hyperfine "perpendicular" ^{31}P couplings ($T_{\perp 1,2}=A_{iso}+\tau_{1,2}=16.3$ and -18.6 G), together with the *g* anisotropy and the small coupling with an additional spin 1/2 nucleus, afford a complex central part whose intensity is similar to the signals A1 and A2.[14] Comparison of these hyperfine tensors with the ^{31}P atomic constants yields the spin densities reported in Table 4.[15]

Upon increasing the temperature to 290 K, a well-resolved doublet of doublets whose parameters are also given in Table 4 was obtained. This spectrum is very similar to that shown for **2** in Figure 3b. The *g* value measured in liquid solution (2.0081) was very similar to the average value obtained from the simulation of the frozen solution spectrum (2.0066). The temperature dependence of the spectrum was found to be reversible.

Table 4. Experimental EPR parameters obtained for a solution of **1** reduced on a potassium mirror in the absence of cryptand.

g tensor	^{31}P coupling [Gauss]	^{1}H coupling [Gauss]	phosphorus spin densities
	$A_{iso}=39.5$[a] and 45.8[b]	$\lvert A_{iso}\rvert=5.6$[a] and 2.3[b]	$\rho_s=0.009$
2.0033	$\tau_1=-29.5$	$\tau_1=-8.7$	$\rho_p=0.37$
2.0106	$\tau_2=-64.4$	$\tau_2=0.3$	
2.0058	$\tau_3=94.1$	$\tau_3=8.4$	

[a] In liquid solution. [b] In frozen solution.

*Reduction of **1** at 200 K on a potassium (or sodium) mirror in the presence of cryptand or by reaction with sodium naphthalenide*: The spectrum shown in Figure 5a was recorded at 200 K after a solution of **1** in THF was allowed to react on a potassium mirror in the presence of cryptand. Any increase in temperature between the time when the reduction was carried out and the EPR spectra were recorded was carefully avoided. In contrast to the doublet of doublets obtained

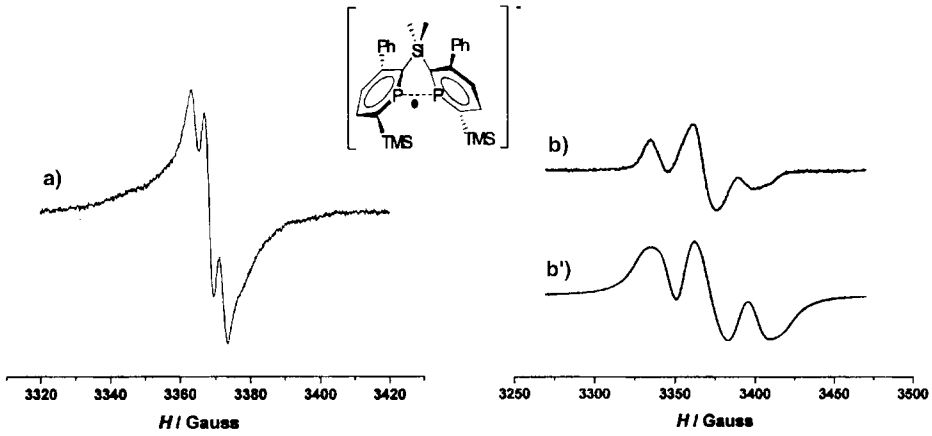

Figure 5. EPR spectra obtained after reduction of a solution of **1** at 200 K on a potassium mirror in the presence of cryptand: a) liquid solution spectrum (200 K); b) frozen solution spectrum (100 K); and b′) spectrum simulated by using the dipolar couplings obtained from DFT calculations.

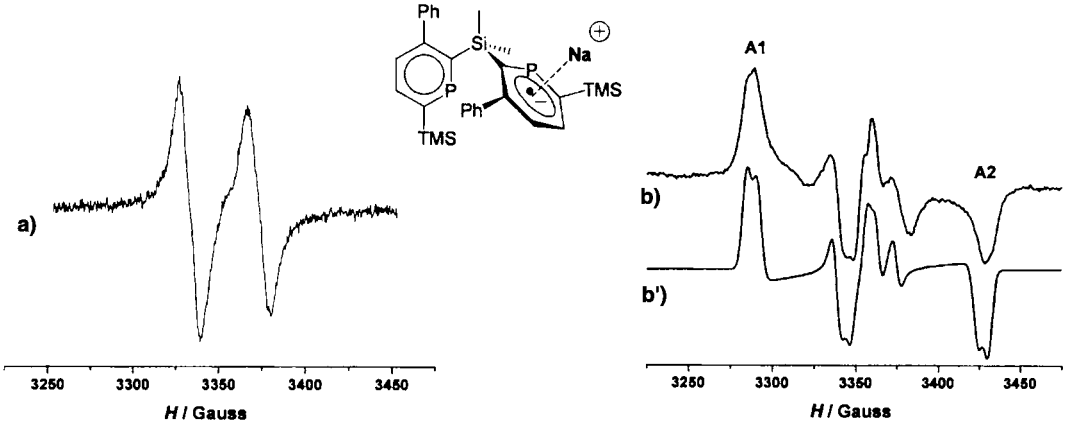

Figure 4. EPR spectra obtained after reduction of a solution of **1** at 200 K on a potassium mirror in the absence of cryptand: a) spectrum recorded at 200 K; b) frozen solution spectrum (95 K); and b′) simulated spectrum.

when the reaction was carried out with alkali metal in absence of cryptand, this spectrum consisted of a triplet with a small coupling constant ($A_{iso} = 4$ G).

When the temperature was decreased to 100 K, an asymmetric triplet (Figure 5b) with a large splitting (~38 G) was obtained. As explained in the DFT section (vide infra), this type of spectrum can be simulated (Figure 5b′) by using the dipolar hyperfine tensors calculated for the bis(phosphinine) radical anion $\mathbf{1'}^{\bullet-}$ (**1′** corresponds to **1** without the phenyl rings). Upon warming the solution once again to 200 K, the same spectrum as that shown in Figure 5a was obtained. However, after one minute at 220 K additional signals appear and the spectrum rapidly becomes complex. These modifications were found to be irreversible and indicate that the compound had undergone partial decomposition.

Very similar spectra were obtained at 100 K when sodium naphthalenide was used, at 200 K, as a reducing agent instead of a "potassium mirror and cryptand".[10]

*Reduction of **1** on a potassium mirror at 298 K and fast cooling to 200 K*: The spectrum shown in Figure 6a was obtained after a THF solution of **1** was allowed to react on a potassium mirror at 298 K in the absence of cryptand and was subsequently rapidly cooled to 200 K. The spectrum exhibits the two patterns observed in Figure 3b and Figure 5a, respectively. In particular, it contains a doublet of doublets, and in the central part, a triplet with a splitting of 4 G. Upon decreasing the temperature to 100 K, a spectrum (Figure 6b) that was practically identical to that observed for the frozen solution of **1** after it had been reduced at 200 K on a potassium mirror in the presence of cryptand or with naphthalenide (Figure 5b) was obtained. As a result of the low intensity of the "parallel" transitions, the external lines marked A1 and A2 in Figure 4a are not detected in Figure 6b.[16] Subsequent warming of the solution afforded the original spectrum observed at 200 K (Figure 6a), but above 220 K new signals appeared that indicated the formation of secondary radical species. As observed above, these transformations were found to be irreversible.

DFT structures of neutral and anionic mono and bis(phosphinines)

Monophosphinine 2 and its radical anion: The optimized structures of **2** and $\mathbf{2}^{\bullet-}$ show that addition of an electron to **2** causes an increase in the P1–C5 ($\Delta = 0.06$ Å) and C1–P1 ($\Delta = 0.09$ Å) bond lengths, and a small shortening of the C1–C2 ($\Delta = -0.02$ Å) and C4–C5 ($\Delta = -0.01$ Å) bonds in accord with the π* character of the SOMO shown in Figure 7

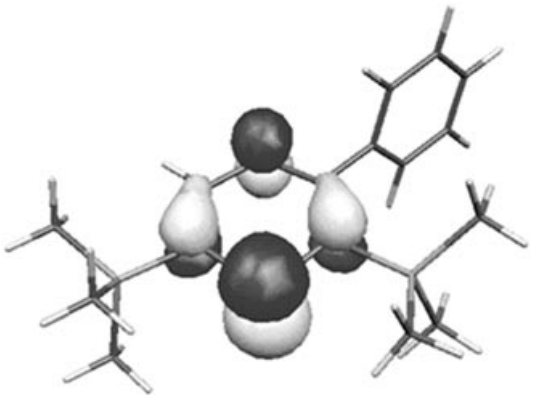

Figure 7. Representation of the SOMO in $\mathbf{2}^{\bullet-}$.

In the radical anion $\mathbf{2}^{\bullet-}$, the phosphinine is almost planar (C3-C2-C1-P1 1.8°, C5-C4-C3-C2 −2.9°) and makes an angle of 102° with the plane of the phenyl ring. The presence of the phenyl group does not appreciably modify the spin densities previously reported for the methylphosphinine radical anion.[5] The isotropic and anisotropic coupling constants for ^{31}P and for the proton located *para* to the phosphorus atom are given in Table 5 along with some gross orbital spin populations. As expected, the ^{31}P isotropic coupling constants calculated with the TZVP basis set are larger than those calculated with the 6-31G* basis set and

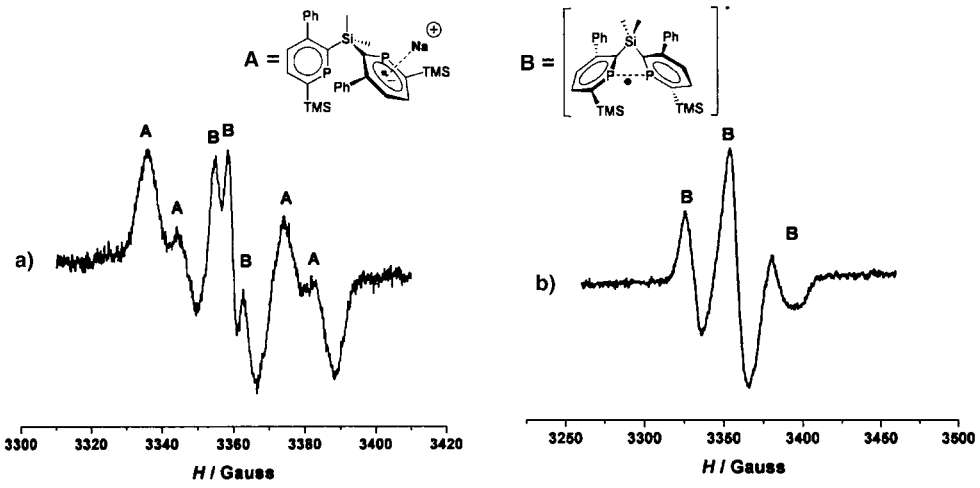

Figure 6. EPR spectra obtained after reduction of a solution of **1** at room temperature on a potassium mirror in the absence of cryptand: a) liquid solution spectrum (200 K); and b) frozen solution spectrum (100 K).

Table 5. DFT calculated coupling constants and spin densities for $2^{\bullet-}$.

Basis set	Hyperfine couplings [Gauss]				Spin densities[a]	
	^{31}P		^{1}H (*para*)		phosphorus p_π	carbon (*para*) p_π
	isotropic	anisotropic	isotropic	anisotropic		
6-31+G*	26	−53, −49, 102	−6.6	−3.5, 0.0, 3.5	0.48	0.27
TZVP	33	−56, −59, 115	−6.0	−3.8, 0.3, 3.5	0.53	0.24

[a] From gross orbital spin populations.

are in reasonable accord with the splitting observed in the EPR spectrum recorded above 245 K (Figure 3b).

On the hypothesis that the *g* tensor is isotropic, the hyperfine tensors calculated with the TZVP basis set give rise to the spectrum shown in Figure 8. The spectrum is composed

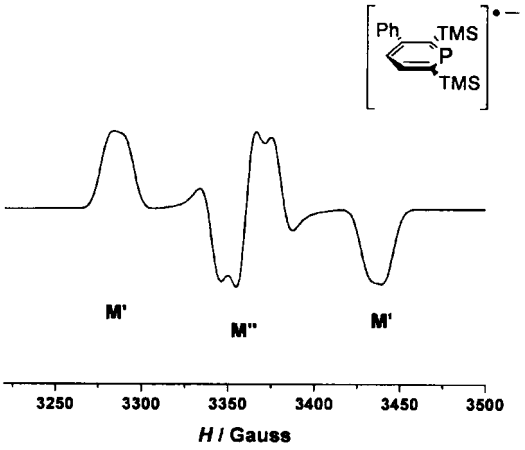

Figure 8. Simulation of the EPR powder spectrum using the DFT calculated hyperfine tensors for $2^{\bullet-}$ and an isotropic *g* tensor ($g = 2.0023$).

of two external lines (marked M′) separated by ~128 G and a central band (marked M″) whose intensity is similar to that of the external lines. An axial distortion of *g* (with $g_\parallel$ aligned along ^{31}P–$T_\parallel$) would cause a broadening of M″ and a decrease in the intensity ratio M″/M′. Although the positions and shapes of the M′ lines are similar to A in the experimentally obtained spectrum (Figure 3a), the central M″ pattern is different from B in Figure 3a.

Phosphinine 1 and its radical anion: Compound **1** is far too large to expect quantitative results from the available nonempirical methods. Therefore, DFT calculations were carried out on the model system **1′**, in which the phosphinine ring does not contain a phenyl group. The purpose of these calculations is to assess to what extent the relative orientation of the two phosphinine rings can lead to hyperfine interactions consistent with the experimental results.

Ion pair 1′$^{-}$Na^{+}: As shown in Figure 9a, we first attempted to estimate the hyperfine couplings for an ion pair when a sodium atom was located in close proximity to one of the two phosphinine rings in **1′**. The hyperfine tensors and the SOMO were obtained from a single-point calculation performed for a conformation of **1′** that was very similar to that obtained for the crystal structure of **1** (see Experimental Section).

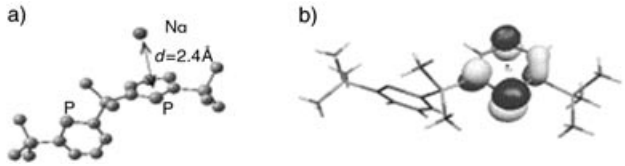

Figure 9. Ion pair $1'^{-}Na^{+}$: a) geometry used to calculate the hyperfine tensors; and b) representation of the SOMO.

When $d = 2.4$ Å (d = distance between the ring and the sodium atom), a Mulliken analysis clearly indicates that a charge separation occurs. Positively charged regions are centered on the sodium atoms, and to a smaller extent on the silicon atoms, while the negatively charged region is mainly located on the phosphinine ring closest to the sodium atom. As shown by the SOMO illustrated in Figure 9b, the unpaired electron is principally localized on that particular phosphinine ring and is reminiscent of the SOMO reported for $2^{\bullet-}$ (Figure 7). The isotropic and anisotropic hyperfine constants are given in Table 6. The ^{31}P and ^{1}H (*para*) couplings are similar to those calculated for $2^{\bullet-}$ as well as to the experimental values measured upon reduction of **1** on a sodium or potassium mirror in the absence of cryptand. The accord between experimental and calculated ^{31}P couplings is slightly better with the TZVP basis set. The single discrepancy lies in the calculated isotropic ^{23}Na coupling which is rather large (10 G) but not actually detected. Nevertheless, taking into account the somewhat arbitrary location of the sodium atom in these DFT calculations, it can be concluded that the spectra shown in Figure 4 do not conflict with the formation of a $[\mathbf{1}]^{-}Na^{+}$ ion pair. The ability of the phosphinine ring to form a tight ion pair has already been reported for disilylphosphinines that bear two methyl groups *meta* to the phosphorus atom.[5] In that particular example the approach of the sodium cation was not hindered either by a

Table 6. EPR parameters for the ion pair $\mathbf{1}'^{\bullet-}Na^{+}$.

Basis set	Hyperfine couplings [Gauss]				Spin densities[a]	
	^{31}P		^{1}H (*para*)		phosphorus p_π	carbon (*para*) p_π
	isotropic	anisotropic	isotropic	anisotropic		
6-31+G*	10	−39, −35, 74	−8	−6, 0, 6	0.41	0.34
TZVP	18	−42, −38, 81	−8.5	−6, 0, 6	0.33	0.36

[a] From gross orbital spin populations.

phenyl group or the second phosphinine ring, and a coupling with ^{23}Na was observed.

Isolated radical anion $\mathbf{1'}^{\bullet-}$: The geometry of the radical anion $\mathbf{1'}^{\bullet-}$ was optimized by using the geometry obtained from the crystal structure of dianion $\mathbf{1}^{2-}$ as an initial conformation. The resultant optimized conformation is shown in Figure 10a, while the corresponding parameters, together with those optimized for $\mathbf{1'}^{2-}$, are reported in Table 7.

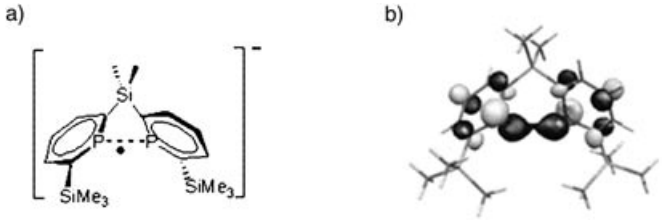

Figure 10. a) Schematic representation of the conformation of $\mathbf{1'}^{\bullet-}$; and b) SOMO for $\mathbf{1'}^{\bullet-}$.

Table 7. Local minima for $[\mathbf{1'}]^{-}$ and $[\mathbf{1'}]^{2-}$.

Radical ion	P1···P2 [Å]	C5–Si2–C6 [°]	C–P–C [°]	ξ[a] [°]
$\mathbf{1'}^{\bullet-}$	3.479	108.74	102.0	62.6
$\mathbf{1'}^{2-}$	2.582	100.99	99.4	44.75
$\mathbf{1}^{2-}$ (experimental)	2.386	98.96	102.7	48.2

[a] ξ = angle formed by the normals to the two C–P–C planes.

Although the model dianion does not contain phenyl substituents, the optimized parameters for $\mathbf{1'}^{2-}$ are consistent with those obtained from the crystal structure of $\mathbf{1}^{2-}$. However, it should be noted that the optimized geometries of the mono and dianion species contain some notable differences. The addition of a second electron to the system shortens the P···P distance by 0.9 Å and decreases the interphosphinine C5–Si–C6 angle by 8°. Moreover, the angle between the normals to the two C–P–C planes decreases by 20°. The SOMO for $\mathbf{1'}^{\bullet-}$ is shown in Figure 10b and clearly shows the bonding overlap between the two phosphorus $3p_\pi$ orbitals, which contain 58% of the spin. The remainder is delocalized on the *ortho* and *para* carbons of the two phosphinine rings. A natural bond orbital study (NBO[17]) carried out (B3LYP functional/TZVP basis set) for this optimized geometry determined that the occupancy of the P–P bond is equal to 0.93 electron.

The dipolar and isotropic couplings calculated for $\mathbf{1'}^{\bullet-}$ are given in Table 8. Since Fermi contact is generally more difficult to predict than dipolar couplings when spin polarization effects are likely to occur, consistency between calculated and experimental data will mainly be based on the contribution of the anisotropic couplings. As shown in Figure 6b, the spectrum simulated by adjusting the g tensor when the calculated dipolar tensors and experimental A_{iso} values (liquid solution) were used is very similar to the experimental frozen solution spectrum.[18] Moreover, the average value of g is very similar to the value measured in liquid solution.

Table 8. Calculated anisotropic (τ) and isotropic (A_{iso}) hyperfine couplings [Gauss] for $\mathbf{1'}^{\bullet-}$ and the adjusted g tensors.

P1 and P2 couplings				H_a (*para*) and H_b (*para*) couplings				Adjusted g tensor
eigenvalues	eigenvectors			eigenvalues	eigenvectors			
	λ	μ	ν		λ	μ	ν	
$\tau_i = -20.6$	0.643	(±)0.765	−0.043	$\tau'_i = -2.24$	0.589	(±)0.804	−0.073	$g_x = 2.0070$
$\tau_j = -22.9$	−0.554	(±)0.426	−0.716	$\tau'_j = -0.06$	−0.596	(±)0.494	0.634	$g_y = 2.0030$
$\tau_k = 43.5$	0.529	(±)0.484	−0.697	$\tau'_k = 2.3$	0.546	(±)0.330	0.770	$g_z = 2.0007$
$A_{iso} = 5$				$A_{iso} = -4$				

Discussion

Before discussing the reduction behavior of system **1** in which the two phosphinine rings are linked by a single O–Si–O chain, it is worthwhile recalling the results[5] previously obtained for compound **3**, which contains two phosphinines linked by two O–Si–O chains, and interpreting the EPR spectra described above for system **2**, which contains a single phosphinine ring. As previously reported in reference [5], reduction of **3** at room temperature readily afforded a rather persistent radical anion whose EPR spectrum was characterized by an isotropic coupling of ≈4 G between two equivalent ^{31}P nuclei. At 120 K the frozen solution spectrum could be simulated by using two aligned ^{31}P coupling tensors ($T_x = -20.4$ G, $T_y = -31.4$ G, $T_z = 40.9$ G) and a g tensor ($g_x = 2.0097$, $g_y = 2.0088$, $g_z = 2.0039$). The DFT calculations for the radical anion $\mathbf{3}^{\bullet-}$ were fully consistent with the experimental tensors. In the reduced species, the SOMO is delocalized over the two phosphinine rings and a one-electron P–P bond is formed by the axial overlap of the two phosphorus p_π orbitals.

The DFT calculations for $\mathbf{2}^{\bullet-}$ (Table 5) determined the ^{31}P couplings to be appreciably larger than those measured for $\mathbf{3}^{\bullet-}$, but were consistent with the doublet of doublets obtained for compound **2** in the liquid phase (Figure 3b). However, for the frozen solutions, whereas the two external signals (marked A on Figure 3a) corresponded to the external lines (M′) predicted by DFT calculations (Figure 8), the intense central part (triplet marked B) was clearly different. In fact, the central triplet B, which exhibits a hyperfine splitting of 30 G with two spin 1/2 nuclei, corresponds well with the frozen solution spectrum expected for a radical such as $\mathbf{3}^{\bullet-}$. This indicates that in the aggregation process that occurs upon a decrease in temperature, an appreciable amount of the radical anions $\mathbf{2}^{\bullet-}$ react with neutral monophosphinines to form weak one-electron P–P bonds to give $[\mathbf{2}_2]^{\bullet-}$. As shown by EPR experiments at various temperatures, the formation of this intermolecular bond is reversible. As is consistent with NMR spectra, further reduction of this radical monoanion leads to the formation of a classical diphosphine bond to give $[\mathbf{2}_2]^{2-}$.

We can now interpret the results obtained for the system that contains a single interphosphinine link. In the liquid phase, reduction of **1** by reaction at 200 K on a potassium or sodium mirror leads to a doublet of

doublets that is similar to the one recorded upon reduction of **2** (Figure 3b), and in which the radical anion is localized on a single phosphinine ring. Additional signals are not observed between 190 and 290 K. Furthermore, the frozen solution spectrum (Figure 4a) also corresponds to this species. In contrast, when compound **1** is reduced on an alkali mirror in the presence of cryptand, the EPR spectrum corresponds to a species which contains a one-electron P–P bond [triplet with small hyperfine couplings in the liquid phase (Figure 5a) and a broad asymmetric spectrum with a splitting of ~30 G at 100 K (Figure 5b)]. Above 210 K the spectrum progressively becomes more complex and several lines appear. Reduction of **1** with sodium (or potassium) naphthalenide at 200 K gives rise to the same spectra as those reported when reduction occurs on a potassium mirror in the presence of cryptand at temperatures below 210 K. Only signals similar to those observed for $\mathbf{3}^{\bullet-}$ are observed. A simple way to rationalize these results is to assume that at low temperatures (<200 K) compound **1** adopts a conformation in which the two phosphorus atoms are far apart (in accord with the crystal structure). Therefore, when the electron transfer occurs under conditions which do not lead to the formation of a tight ion pair between an alkali cation and a phosphinine anion (e.g. electron transfer between naphthalenide and the phosphinine moiety, or reduction with an alkali mirror in the presence of cryptand), an electron passes from the reducing agent to one of the two phosphinine rings and the system immediately relaxes and undergoes further modifications. In particular, the C–Si bond undergoes internal rotation, the unpaired electron on the two phosphinine rings is delocalized, and subsequently a one-electron P–P bond is formed (Scheme 3).

The angle between the two calculated ^{31}P-$\tau_{\parallel}$ eigenvectors (~60°) indicates a modest overlap between the two p orbitals. Therefore, the phosphorus–phosphorus interaction is rather weak. Indeed, this occurs because of the cyclic constraint imposed by the interphosphinine link shown in $[\mathbf{1}]^{2-}\cdot 2\,Na^{+}$. This radical anion is, in fact, an intermediate which subsequently goes on to form a "classical" P–P bond upon being reduced by a second electron. However, in contrast to the reaction that occurs with naphthalenide, when the reduction is performed by directly transferring an electron from the alkali metal to the phosphinine, a countercation (K^+ or Na^+) is immediately formed in the vicinity of the reduced phosphinine ring. Then, if cryptand is absent, a tight ion pair is formed; this stabilizes the radical anion localized on a single phosphinine ring, hinders internal rotation, and prevents the formation of a P–P bond. This proposed mechanism is consistent with the spectra obtained when a solution of **1** at room temperature is allowed to react only briefly, and the spectra are rapidly recorded at 200 K. Under these conditions, at the time when the electron transfer occurs, several conformations of **1** probably coexist in solution. Those with a short P···P distance are likely to give rise to a P–P bond (triplet with a small splitting), while those with a large P···P distance give rise to the localized radical anion (doublet of doublet). Figure 6a clearly exhibits these two contributions in the spectrum recorded in the liquid phase. When the solution is frozen only the signals due to the delocalized species are detected, those due to the localized anion are expected to be considerably smaller since only the external weak "parallel" transitions could be observed. Although there are not many alternatives to the mechanism shown in Scheme 3 which would explain the spectra observed when alkali mirrors are used as reductants, in instances when naphthalenide anions are used as reductants, we cannot exclude that the naphthalene ring favors the formation of the one-electron P–P bond by participating in the electron-transfer transition state.

It is worth noting that in contrast to the localized radical anion (e.g. $Na^{+}\mathbf{1}^{\bullet-}$), which is stable at room temperature, or to the delocalized anion $\mathbf{3}^{\bullet-}$, the delocalized species $\mathbf{1}^{\bullet-}$ rapidly undergoes decomposition above 210 K to give secondary radical species. This probably explains why it is almost impossible to obtain clear and unambiguous spectra of the electrochemical reduction of **1**. A triplet is indeed formed immediately after electrolysis is begun at 200 K, but it is quickly accompanied by several species that have larger couplings.

Conclusion

The EPR spectra obtained for the reduction of a system that bears two phosphinine rings clearly show that when two equivalent reduction centers are present the reduction process is affected by the relative orientation of the two electron-acceptor sites. Therefore, some of the factors that govern the electron-transfer mechanism include: the presence of cumbersome substituents that hinder internal rotations and prevent the molecule from adopting certain conformations; temperature, which determines the equilibrium between various rotamers; the presence of

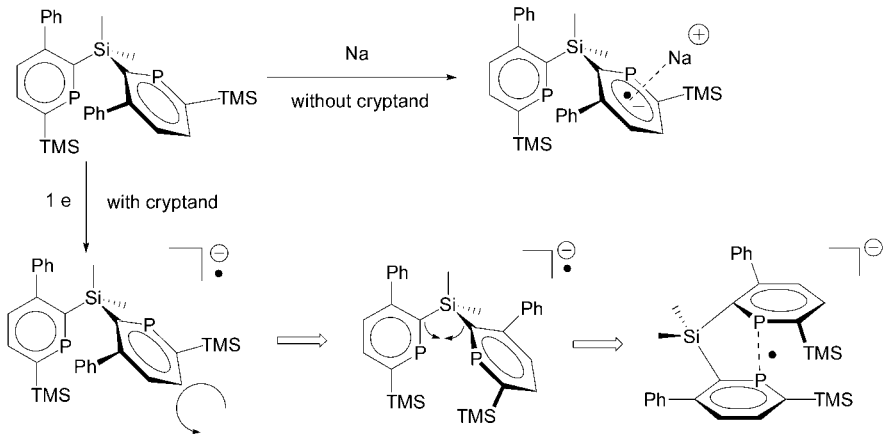

Scheme 3. Proposed pathways for the formation of the bis(phosphinine) monoanion.

metal ions which can form ion pairs and stabilize a particular structure; and the presence of cage molecules or chelating agents which preclude the formation of ion pairs. All these factors are likely to be involved in many biological systems and to participate in the regulation of electron-transfer processes.

Experimental Section

All syntheses were carried out under an inert atmosphere using Schlenk techniques.

Compounds: Bis(3-phenyl-6–6(trimethylsilyl)phosphinine-2-yl)dimethylsilane (**1**) was synthesized according to a previously reported method.[9]

2,6-Bis(trimethylsilyl-3-phenylphosphinine) (2): A solution of diazaphosphinine[8] (0.38 g, 1.8 mmol) and phenyl trimethylsilyl acetylene (280 μL, 1.8 mmol) in toluene (12 mL) was stirred at 65 °C while the reaction was followed by ^{31}P NMR spectroscopy. Formation of azaphosphinine (δ = 303.9 ppm, s) was complete after 18 h. Trimethylsilyl acetylene (1.3 mL, 9.2 mmol, 5 equiv) was then added and the solution was heated for a further 5 h at 90 °C. The solution was cooled to room temperature, celite (1 g) was added, and toluene was removed in vacuo. The resultant phosphinine was purified by chromatography using hexane as eluent. The first fraction contained 2,6-bis(trimethylsilylphosphinine), while the desired product was in the second fraction. Upon removal of the solvent, the product was isolated as a white powder. Yield: 285 mg (50 %); ^{1}H NMR ($CDCl_3$, 300 MHz): δ = 0.08 and 0.41 (2 s, 18 H; $Si(CH_3)_3$), 7.25–7.44 (m, 6 H; C_6H_5 and C_4H), 8.07 ppm (t, J(H,H) = J(H,P) = 8.8 Hz, 1 H; C_5H); ^{13}C NMR ($CDCl_3$, 75.5 MHz): δ = 0.2 (d, J(C,P) = 5.8 Hz; $Si(CH_3)_3$), 2.2 (d, J(C,P) = 10.3 Hz; $Si(CH_3)_3$), 127.5, 127.9, and 129.1 (3 s; C_6H_5), 129.4 (d, J(C,P) = 24.3 Hz; C_4H), 138.1 (d, J(C,P) = 10.1 Hz; C_5H), 146.0 (d, J(C,P) = 9.0 Hz; *ipso*-C of C_6H_5), 153.7 (d, J(C,P) = 12.5 Hz; C_3 in C_6H_5), 168.0 and 168.3 ppm (2 d, J(C,P) = 91.7 and 83.8 Hz; C_2-TMS); ^{31}P NMR (CH_2Cl_2, 121.5 MHz): δ = 261.6 ppm (s); elemental analysis calcd (%) for $C_{17}H_{25}PSi_2$ (316.53): C 64.51, H 7.96; found: C 64.70, H 8.21.

Chemical reductions

*Reduction of **1***: To a solution of bis-phosphinine (25 mg, 0.046 mmol) in THF (1 mL) at room temperature was added a solution of sodium naphthalenide (0.9 mL, 0.046 mmol, 50 mM in THF). The color of the reaction mixture immediately changed to burgundy red. The solvent was removed in vacuo and the product was isolated as a very moisture sensitive brown powder. ^{1}H NMR ([D_8]THF, 300 MHz): δ = −0.85 (s, 6 H; $Si(CH_3)_2$), 0.12 (s, 18 H; $Si(CH_3)_3$), 3.94 (d, J(H,H) = 7.7 Hz, 2 H; C_4H), 6.13 (dt, J(H,H) = 7.5 Hz, J(H,P) = 6.4 Hz, 2 H; C_5H), 7.09–7.16 ppm (m, 10 H; C_6H_5); ^{13}C NMR ([D_8]THF, 75.5 MHz): δ = −0.9 (s, $Si(CH_3)_2$), 1.7 (s, $Si(CH_3)_3$), 90.8 (t, J(C,P) = 9.5 Hz; C_2 in $Si(CH_3)_2$), 96.2 (t, J(C,P) = 28.1 Hz; C_6 in $Si(CH_3)_3$), 98.6 (t, J(C,P) = 7.9 Hz; C_4H), 126.4–130.6 (m, C_6H_5), 147.25 (s, C_5H), 152.0 (s, *ipso*-C of C_6H_5), 162.6 ppm (s, C_3Ph); ^{31}P NMR (THF, 121.5 MHz): δ = 22.0 ppm (s).

*Reduction of **2***: To a solution of phosphinine (34.2 mg, 0.11 mmol) in THF (1 mL) at room temperature was added a solution of sodium naphthalenide (1.1 mL, 0.11 mmol, 0.1 M in THF). The color of the reaction mixture immediately changed to dark green. The solvent was removed in vacuo and the product was isolated as a very moisture sensitive green powder. NMR spectroscopy revealed that the solution was a mixture of *cis* and *trans* isomers (1:4). ^{1}H NMR ([D_8]THF, 300 MHz): δ = −0.21 (s, 4.5 H; $Si(CH_3)_3$ minor), −0.15 (s, 18 H; $Si(CH_3)_3$ major), 0.11 (s, 18 H; $Si(CH_3)_3$ major), 0.15 (s, 4.5 H; $Si(CH_3)_3$ minor), 5.21 (d, J(H,P) = 6.5 Hz, 0.5 H; C_4H minor), 5.25 (d, J(H,P) = 6.8 Hz, 2 H; C_4H major), 7.00–7.30 (m, 12.5 H; C_6H_5), 7.56 (d, J(H,P) = 6.4 Hz, 0.5 H; C_3H minor), 7.65 ppm (d, J(H,P) = 6.3 Hz, 2 H; C_3H major); ^{13}C NMR ([D_8]THF, 75.5 MHz): δ = 0.4, 2.0, 3.6, 6.7 (4 s, $Si(CH_3)_3$), 102.7 (s, C_4H), 128.1 (s, *ipso*-C of C_6H_5), 128.8 (s, C_3 of C_6H_5), 133.1 (s, C_5H), 146.2 (s, C_2 of C_6H_5), 152.2 (s, C_1 of C_6H_5), 160.7 ppm (s, C_3 of C_6H_5); ^{31}P NMR (THF, 121.5 MHz): δ = −82.8 (br s, major product), −77.12 ppm (br s, minor product).

Crystallization and crystal structures: Single crystals of compound **1** suitable for crystallography were obtained by diffusing methanol into a toluene solution of the compound. Single crystals of compound $[\mathbf{1}]^{2-}\cdot 2\,Na^+$ were obtained by slow recrystallization from a mixture of diethyl ether and THF (1:1) at −18 °C in a tube sealed under vacuum. CCDC-228879 and CCDC-228880 contain the supplementary crystallographic data for this paper. These data can be obtained free of charge via www.ccdc.cam.ac.uk/conts/retrieving.html (or from the Cambridge Crystallographic Data Centre, 12 Union Road, Cambridge CB2 1EZ, UK; fax: (+44) 1223-336-033; or e-mail: deposit@ccdc.cam.ac.uk).

EPR measurements: EPR spectra were recorded on a Bruker 200D-SRC or a Bruker ESP-300 spectrometer (X-band, 100 kHz field modulation) equipped with a Bruker ER-4111 VT and an ER-081S variable temperature controller, respectively. Freshly distilled THF was used as a solvent, and the solutions were carefully degassed on a vacuum line. Potassium and sodium mirrors were formed by sublimation of the metal under high vacuum (10^{-6} Torr). Reduction reactions on mirrors were carried out under vacuum in sealed tubes. Chemical reductions with sodium naphthalenide were performed under an atmosphere of nitrogen.

DFT calculations: Spin-unrestricted calculations were carried out with the Gaussian 98 and Gaussian 03[19] packages using the B3LYP functional.[20] Geometries for the neutral systems (**1′**, **2**) were optimized using the 6-31G* basis set functions. The geometry of $\mathbf{1'}^{\cdot-}$ was optimized using the 6-31+G* basis set, while the hyperfine couplings and molecular orbitals were calculated using the 6-31+G* and TZVP[21] functions. The 6-31+G* and TZVP basis sets were also used for optimization and calculation of the properties of the radical anion $\mathbf{2}^{\cdot-}$.

Calculations for $\mathbf{1'}^{\cdot-}Na^+$ were carried out on **1′**Na, and it was assumed that except for the phosphinine ring close to the sodium atom, which was assumed to adopt the geometry previously optimized[10] (B3LYP//6-31+G$^+$) for the phosphinine radical anion $(C_5PH_5)^-$, **1′** would adopt the conformation optimized for molecule **1**. The sodium atom was placed in the symmetry plane of the C_5PH_5 ring, which was kept fixed in a slight "boat" deformation. Calculations were performed for several Na···P distances (d) and for various distances (L) between sodium and the plane formed by the *ortho* and *meta* carbon atoms. The minimum energy was found to occur when d = 2.25 Å and L = 2.4 Å. The hyperfine tensors and SOMO were calculated for this geometry using either the 6-31+G$^+$ or the TZVP basis set for phosphorus, while for all other atoms the 6-31+G$^+$ basis set was used.

The Molekel program[22] was used to represent the molecular orbitals.

Acknowledgments

This work was supported by the CNRS and the Ecole Polytechnique (Palaiseau). The authors would like to thank IDRIS (Paris XI Orsay University, France) for the allowance of computer time. Support of this work by the Swiss National Science Foundation and the Swiss Center for Scientific Computing is gratefully acknowledged.

[1] a) D. Astruc, in *Electron Transfer and Radical Processes in Transition-Metal Chemistry*, Wiley-VCH, **1995**, New York; b) Z. V. Todres, *Organic Ion Radicals*, Marcel Dekker, **2003**, New York.

[2] a) A. E. Kaifer, M. Gomez-Kaifer, in *Supramolecular Electrochemistry*, Wiley-VCH, **1999**, Weinheim; b) J.-P Sauvage, *Molecular Machines and Motors*, Springer, **2001**, Berlin.

[3] a) M. Szwarc, *Acc. Chem. Res.* **1969**, *2*, 87–96; b) M. Szwarc, *Acc. Chem. Res.* **1972**, *5*, 169–176; c) H. Bock, M. Ansari, N. Nagel, Z. Havlas, *J. Organometallic Chem.* **1995**, *499*, 63–71; d) C. Näther, H. Bock, Z. Havlas, T. Hauck, *Organometallics* **1998**, *17*, 4707–4715; e) T. Nishinaga, D. Yamasaki, H. Stahr, A. Wakamiya, K. Komatsu, *J. Am. Chem. Soc.* **2003**, *125*, 7324–7335; f) P. B. Hitchkock, M. F. Lappert, A. V. Protchenko, *J. Am. Chem. Soc.* **2001**, *123*, 189–190.

[4] C. Dutan, S. Choua, T. Berclaz, M. Geoffroy, N. Mézailles, A. Moores, L. Ricard, P. Le Floch, *J. Am. Chem. Soc.* **2003**, *125*, 4487–4494.

[5] L. Cataldo, S. Choua, T. Berclaz, M. Geoffroy, N. Mézailles, L. Ricard, F. Mathey, P. Le Floch, *J. Am. Chem. Soc.* **2001**, *123*, 6654–6661.

[6] For other odd-electron bonds studies see: Y. Canac, D. Bourissou, A. Baceiredo, H. Gornitzka, W. W. Scholer, G. Bertrand, *Science* **1998**, *279*, 2080–2082; H. Grützmacher, F. Breher, *Angew. Chem.* **2002**, *114*, 4178–4184; *Angew. Chem. Int. Ed.* **2002**, *41*, 4006–4011.
[7] J. D. Hoefelmeyer, F. P. Gabbaï, *J. Am. Chem. Soc.* **2000** *122*, 9054–9055.
[8] N. Avarvari, P. Le Floch, F. Mathey, *J. Am. Chem. Soc.* **1996**, *118*, 11978–11979.
[9] N. Avarvari, P. Le Floch, L. Ricard, F. Mathey, *Organometallics* **1997**, *16*, 4089–4098.
[10] See Supporting Information.
[11] Additional experiments showed that the intensity ratio (A/B) measured on the frozen solution spectra was sensitive to additional factors such as the concentration ratio of sodium naphthalenide/phosphinine **2**.
[12] At 100 K, only the B lines in Figure 3a were observed after reduction was carried out with sodium naphthalenide in the absence of cryptand. Although a frozen solution spectrum could not be clearly recorded upon reduction of **2** with a sodium mirror, a broad doublet (40 G) was observed at 200 K. The signals observed upon reduction with naphthalenide or alkali metal were also detected after in situ electrolysis of a THF solution of **2** in the EPR cavity. However, with this method additional lines were observed that can tentatively be attributed to protonation of the radical anion by traces of water in the electrolytic cell.
[13] E. Soulié, C. Faure, T. Berclaz, M. Geoffroy, in *Automatic Differentiation of Algorithms*, Springer, New-York **2002**, pp. 99–106.
[14] The drastic diminution of the central part of the frozen solution spectrum as a result of an overlap of the "perpendicular" transitions of an axial ^{31}P tensor is reminiscent of previous observation made for phosphinyl radicals.
[15] J. Morton and K. Preston, *J. Magn. Reson.* **1978**, *30*, 577–582.
[16] We cannot exclude that an intermolecular one-electron P–P bond is not formed in the frozen solution. Such a reaction between a localized radical anion and a neutral phosphinine would decrease the amount of localized radical anions responsible for signals of type A1 and A2.
[17] E. D. Glendening, A. E. Reed, J. E. Carpenter, F. Weinhold. Natural Bond Orbital Analysis, NBO 3.1; Theoretical Chemistry Institute, University of Wisconsin, Madison, WI,
[18] Although the calculated isotropic coupling with the *para* protons is around 4 G, the corresponding splitting is not detected in the spectrum. This can arise either because of a slight difference between the real and calculated geometries (absence of phenyl in the model system) or because of molecular motion, which alters the line shape. When couplings are calculated with a triple zeta basis set the ^{31}P isotropic couplings increase, while the ^{1}H isotropic couplings decrease.
[19] *Gaussian 03*, *Revision B.03*, M. J. Frisch, G. W. Trucks, H. B. Schlegel, G. E. Scuseria, M. A. Robb, J. R. Cheeseman, J. A. Montgomery, Jr., T. Vreven, K. N. Kudin, J. C. Burant, J. M. Millam, S. S. Iyengar, J. Tomasi,V. Barone, B. Mennucci, M. Cossi, G. Scalmani, N. Rega, G. A. Petersson, H. Nakatsuji, M. Hada, M. Ehara, K. Toyota, R. Fukuda, J. Hasegawa, M. Ishida, T. Nakajima, Y. Honda, O. Kitao, H. Nakai, M. Klene, X. Li, J. E. Knox, H. P. Hratchian, J. B. Cross, C. Adamo, J. Jaramillo, R. Gomperts, R. E. Stratmann, O. Yazyev, A. J. Austin, R. Cammi, C. Pomelli, J. W. Ochterski, P. Y. Ayala, K. Morokuma, G. A. Voth, P. Salvador, J. J. Dannenberg, V. G. Zakrzewski, S. Dapprich, A. D. Daniels, M. C. Strain, O. Farkas, D. K. Malick, A. D. Rabuck, K. Raghavachari, J. B. Foresman, J. V. Ortiz, Q. Cui, A. G. Baboul, S. Clifford, J. Cioslowski, B. B. Stefanov, G. Liu, A. Liashenko, P. Piskorz, I. Komaromi, R. L. Martin, D. J. Fox, T. Keith, M. A. Al-Laham, C. Y. Peng, A. Nanayakkara, M. Challacombe, P. M. W. Gill, B. Johnson, W. Chen, M. W. Wong, C. Gonzalez, J. A. Pople, *Gaussian*, *Inc.*, *Pittsburgh PA*, **2003**.
[20] a) A. D. Becke, *J. Chem. Phys.* **1993**, *98*, 5648–5652;b) C. Lee, W. Yang, R. G. Parr, *Phys. Rev.* **1988**, *54*, 785.
[21] N. Godbout, D. R. Salahub, J. Andzelm, E. Wimmer, *Can. J. Chem.* **1992**, *70*, 560.
[22] Flukiger, P. Development of Molecular Graphics Package MOLEKEL, Ph. D. Thesis, University of Geneva, Switzerland, **1992**.

Received: January 21, 2004
Published online: July 5, 2004